Journal of Molecular Liquids 326 (2021) 115349

Contents lists available at ScienceDirect

Journal of Molecular Liquids

journal homepage: www.elsevier.com/locate/molliq

Influence of molecular geometry on the formation, architecture and dynamics of H-bonded supramolecular associates in 1-phenyl alcohols

Andrzej Nowok [a,*], Karolina Jurkiewicz [a,b], Mateusz Dulski [b,c], Hubert Hellwig [d], Jan G. Małecki [d], Katarzyna Grzybowska [a,b], Joanna Grelska [a,b], Sebastian Pawlus [a,b]

[a] Institute of Physics, University of Silesia in Katowice, 75 Pułku Piechoty 1, 41-500 Chorzów, Poland
[b] Silesian Center for Education and Interdisciplinary Research, 75 Pułku Piechoty 1A, 41-500 Chorzów, Poland
[c] Institute of Materials Engineering, University of Silesia in Katowice, 75 Pułku Piechoty 1A, 41-500 Chorzów, Poland
[d] Institute of Chemistry, University of Silesia in Katowice, Szkolna 9, 40-003 Katowice, Poland

A R T I C L E I N F O

Article history:
Received 15 June 2020
Received in revised form 29 December 2020
Accepted 7 January 2021
Available online 12 January 2021

Keywords:
H-bonded supramolecular assembly
Broadband dielectric spectroscopy
Molecular dynamics
Phenyl alcohols
Structural relaxation
Debye process

A B S T R A C T

Combination of calorimetric, dielectric, infrared, diffraction studies and quantum DFT computations was used to analyze the impact of the molecular architecture of a set of four 1-phenyl alcohols (1-phenylethanol, 1-phenyl-1-propanol, 1-phenyl-1-butanol and 2-methyl-1-phenyl-1-propanol) on their glass transition temperature, molecular dynamics, relaxation processes, hydrogen-bonding pattern and intermolecular association. We showed that all these alcohols form H-bonded supramolecular nanoassociates even at room temperature, despite containing a steric hindrance in the form of the phenyl ring in the most disfavored position. However, the concentration and the size of the H-bonded structures as well as the mutual arrangement of molecules in these clusters are tremendously affected by the molecular architecture. In linear-shaped 1-phenyl alcohols, i.e., 1-phenylethanol, 1-phenyl-1-propanol, 1-phenyl-1-butanol, the intermolecular O-H···O bonds organize themselves into chain-like patterns. Moreover, these alcohols are characterized by similar strength of intermolecular H bonds at each temperature and similar glass transition temperature. In turn, the globular molecular shape of 2-methyl-1-phenyl-1-propanol leads to a weakening of H bonds in this system, an increase in the glass transition temperature and the formation of supramolecular clusters in which O-H···O connections imply ring-like organization of molecules. Finally, these studies clearly show that unlike the glass transition temperature, the molecular dynamics of the 1-phenyl alcohols in the liquid state is not only affected by the molecular architecture and hydrogen bond strength but also by the morphology of the associates composed of H-linked molecules.

1. Introduction

Hydrogen bonds are one of the most important inter- and intramolecular interactions which play a crucial role in countless biological and chemical processes and have a decisive impact on the physicochemical properties of a wide range of substances [1–6]. These interactions are also responsible for self-assembly in liquids, leading to the formation of supramolecular aggregates [7–9]. Although such a phenomenon was observed for some van der Waals systems and ionic liquids, self-assembly through H bonding is of particular interest [10–12]. This behavior was observed for a great number of monohydroxy alcohols, which due to structural simplicity and high vitrification ability are believed to be model systems for the studies on the self-assembly phenomena, carried out by means of various techniques, such as broadband dielectric spectroscopy, dynamic and static light scattering, mechanical or vibrational spectroscopy [8,13–15]. It should be emphasized that a unique feature of the dielectric loss spectra of many alcohols is the Debye process, slower than the structural one. According to the transient chain model, the Debye relaxation is strictly connected with reorientational motions of the whole supramolecular structures or attachment and detachment processes of molecules to and from the associates [8,16]. Therefore, in the case of many monohydroxy alcohols, it is possible to follow the molecular dynamics of supramolecular associates in the broad time range by dielectric spectroscopy.

Among many factors affecting the formation, architecture and dynamics of H-bonded self-assemblies (e.g., temperature, pressure, high electric field, concentration, solvent), the molecular structure seems to have a decisive impact [17–21]. Systematic studies on geometric isomers of octanol revealed the generation of the ring- or chain-like supramolecular structures in these liquids, depending on, among others, the architecture of molecules [22–24]. It was stated that isomers sterically hindered by an alkyl substituent tend to form dimers or higher-membered rings. In turn, isomers with less-hindered hydroxyl group

---

* Corresponding author.
E-mail address: andrzej.nowok@smcebi.edu.pl (A. Nowok).

https://doi.org/10.1016/j.molliq.2021.115349
0167-7322/

agglomerate in chain-like associates more likely [22]. Moreover, it was found that linear alcohols (such as n-octanol, n-butanol) organize themselves into chain-like associates, whereas alcohols with molecules of globular shape (such as *tert*-butanol) tend to form ring-like aggregates [25–28]. The phenyl ring is another component of the molecular structure influencing the dynamics of alcohols. This moiety plays a role of a steric hindrance so that the formation of H-bonded supramolecular clusters may be hampered [29,30]. Such a situation leads to the disappearance of the Debye relaxation process as a separate relaxation peak from dielectric spectra. However, pressure evolution of the *steepness* index for 1-phenyl-2-butanol, determined for structural relaxation, shows the characteristic abrupt increase in the value of this parameter, but only after exceeding a critical pressure - similarly to the behavior of monohydroxy alcohols with a well visible Debye process (e.g., 2-ethyl-1-hexanol) [17,31]. Such a pressure behavior of the *steepness* index was ascribed to modifications of the morphology of the H-bonded associates [17]. Moreover, most recent studies on the series of phenyl-substituted propanols, based on the conjunction of broadband dielectric spectroscopy and photon correlation spectroscopy, have indicated that self-assembly through H bonding is possible even for the most sterically disfavored 1-phenyl-1-propanol [32]. It was shown that the dielectric spectra registered for these alcohols above the glass transition temperature, T_g, can be interpreted as a superposition of the structural α-relaxation and the low-frequency Debye process [32]. The architecture of H-bonded supramolecular structures in liquid phenyl-substituted propanols is, however, complex. While 2-phenyl-1-propanol and 3-phenyl-1-propanol form rather chain-like aggregates, there is a temperature-dependent balance between ring- and chain-like configurations of H bonds in the associates in the case of 1-phenyl-1-propanol [32]. Apart from the main relaxation process being a superposition of the structural α-relaxation and the low-frequency Debye mode, also secondary relaxation processes, characterized by the Arrhenius temperature dependence, were detected for 1-phenyl-1-propanol [33].

Based on infrared (IR) spectroscopy studies supported by quantum calculations, 1-phenylethanol was also found to form aggregates, such as dimers, trimers and multimers. However, the degree of association and architecture of the H-bonded supramolecular structures were solvent-dependent [34]. Like other chiral compounds, 1-phenylethanol can adopt various conformations, differentiated in terms of energy and, consequently, stability [34]. Although its predominant, most stable conformer is stabilized by weak intramolecular O-H···π and C-H···O hydrogen bonds, the molecules in the liquid state are involved into the formation of two-coordinated intermolecular H bonding networks, leading to the creation of multimers [34]. Additionally, molecules of 1-phenylethanol may also form intermolecular O-H···π bonds, typical for all phenyl alcohols in the liquid state and visible in the IR spectra as a weak band at 3567 cm^{-1} [34]. Despite numerous studies, there are still many deficiencies in the description of how the molecular structure and the steric hindrance influence the formation and the architecture of the H-bonded supramolecular clusters in phenyl alcohols.

In this article, we study a set of four monohydroxy 1-phenyl alcohols, i.e., 1-phenylethanol, 1-phenyl-1-propanol, 1-phenyl-1-butanol and 2-methyl-1-phenyl-1-propanol, as model H-bonded sterically hindered glass-formers. We analyze how the increase in the length of alkyl chain and the change in the molecular geometry from linear to globular affect their ability to self-assembly through H bonding, molecular dynamics in supercooled liquid and glassy states and glass transition temperature. Furthermore, we discuss the impact of steric hindrance and molecular architecture on the strength of hydrogen bonds and the architecture of the H-bonded supramolecular structures. The studies are based on broadband dielectric (BDS) and Fourier transform infrared (FTIR) spectroscopy, X-ray diffraction (XRD) and density functional theory (DFT) computations.

2. Materials and methods

2.1. Materials

The analyzed set of chemical compounds consists of four monohydroxy alcohols: (*S*)-1-phenylethanol, 1-phenyl-1-propanol, 1-phenyl-1-butanol and 2-methyl-1-phenyl-1-propanol, labeled further as 1P1E, 1P1P, 1P1B and 2M1P1P, respectively. Their chemical structures are shown in Fig. 1a. The two first liquids were purchased from Sigma-Aldrich. 1P1B and 2M1P1P were synthesized by Grignard reaction of benzaldehyde with a proper organomagnesium reagent in dry diethyl ether, that is propylmagnesium bromide and 2-methylpropylmagnesium bromide, respectively. The Grignard reagents were prepared by reaction of corresponding alkyl halides with magnesium, started by the addition of a small amount of elemental iodine. Grignard reactions were followed by standard acidic (HCl) aqueous workup, extraction, and drying of organic phases by anhydrous $MgSO_4$. Raw products were vacuum distilled in Kugelrohr apparatus, purified using column chromatography (SiO_2, DCM-hexane mixture as eluent) and again vacuum distilled to ensure high purity, dryness and lack of silica gel dust contamination. In order to eliminate traces of water from the liquids, each substance was additionally lyophilized prior to measurements. Apart from 1P1E, all other substances were racemic mixtures of both *R* and *S* isomers.

All the analyzed alcohols contain the phenyl ring located at the first carbon atom of the alkyl chain (Fig. 1a). Therefore, this chemical moiety plays the role of a potential steric hindrance for the linkage of molecules into H-bonded associates. Moreover, each alcohol is of the secondary order. The difference between them lies in the number of carbon atoms in the alkyl chain, varying from 2 for 1P1E, through 3 for 1P1P, up to 4 for 1P1B and 2M1P1P. In order to investigate the influence of the molecular architecture on the molecular dynamics and morphology of supramolecular structures, two isomeric alcohols with four carbon alkyl atoms and differentiated only in terms of the position of -CH_3 moiety were probed: 1P1B and 2M1P1P. The alkyl chain is branched in the latter compound, making the hydroxyl group more sterically screened, and contributing to the change in the molecular shape to a nearly globular one (Fig. 1b). In the case of 2M1P1P, the ratio of the long axis of the molecule to the short one takes the value of ~1.4, whereas it grows up to ~2.3 for 1P1B. Therefore, we will call 2M1P1P alcohol as globular one while the others, 1P1E, 1P1P and 1P1B, as linear ones. It should also be emphasized that 2M1P1P is the only possible branched isomer among the 1-phenyl alcohols of secondary order containing four carbon atoms in the alkyl chain.

2.2. Differential scanning calorimetry (DSC)

The calorimetric measurements of the 1-phenyl alcohols were performed with the use of a Mettler-Toledo DSC apparatus equipped with a liquid nitrogen cooling accessory and a HSS8 ceramic sensor (heat flux sensor with 120 thermocouples). Each liquid was poured into a sealed 40 μl aluminium pan. The thermograms were collected during heating runs with a heating rate equal to 10 K/min at the temperature range of 173–298 K. All scans were carried out in the atmosphere of nitrogen with a flow of 60 mL/min. Glass transition temperature for each compound was determined from these measurements as an onset of the proper thermal effect.

Using a stochastic temperature-modulated differential scanning calorimetry (TMDSC) technique implemented by Mettler-Toledo TOPEM®, the dynamic behaviors of the investigated phenyl alcohols have been analyzed in the frequency range from 4 mHz to 20 mHz in

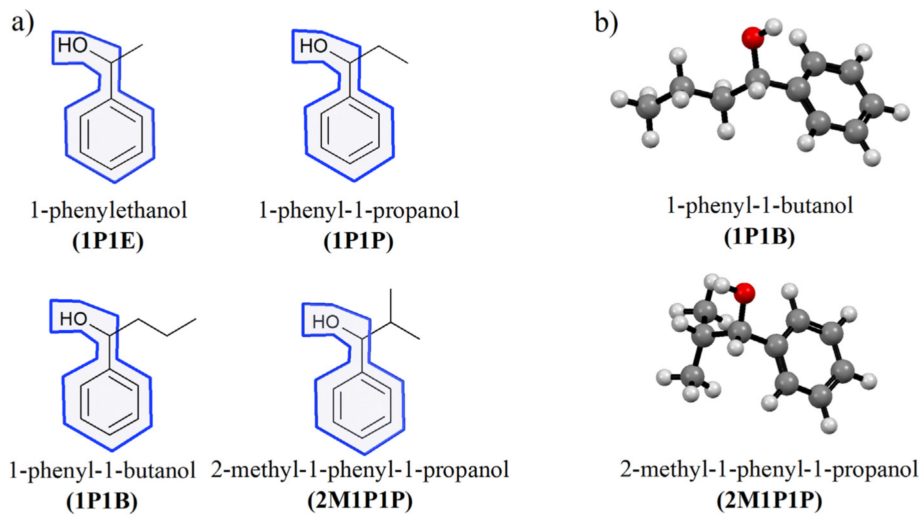

Fig. 1. (a) Overview of the chemical structures for the studied monohydroxy 1-phenyl alcohols. The structural moiety common for all compounds is marked with a blue loop. (b) Comparison of 3D models of 1P1B and 2M1P1P molecules.

one single measurement at a heating rate of 0.5 K/min. In the experiment, a temperature amplitude of the pulses of 0.5 K was selected with a switching time range with minimum and maximum values of 15 and 30 s, respectively. The calorimetric structural relaxation times, $\tau_\alpha = 1/2\pi f$, have been determined from the temperature dependences of the real part of the complex heat capacity, $c_p'(T)$, obtained at different frequencies in the glass transition region for all samples. The glass transition temperature, T_g, was determined for each frequency as the temperature of the half step height of $c_p'(T)$.

2.3. Broadband dielectric spectroscopy (BDS)

Molecular dynamics at ambient pressure of the analyzed set of 1-phenyl alcohols was analyzed by means of broadband dielectric spectroscopy. Each liquid was poured between two parallel plates (of 10 mm diameter, made of stainless steel and distanced with two 100 μm thick glass fibres) of a capacitor, sealed with a Teflon ring. The dielectric measurements were performed over a wide frequency range from 10^{-1} to 10^6 Hz using a Novocontrol Alpha BDS spectrometer equipped with a Quatro Cryosystem. Prior to measurements, each sample was vitrified: in the case of 1P1E, 1P1P and 2M1P1E by cooling with a rate of 10 K/min in the setup or by rapid cooling in liquid nitrogen in the case of 1P1B due to its higher crystallization tendency. The temperature was stabilized by means of nitrogen gas for 2 min before each measurement with a precision better than 0.2 K. The temperature range was different for each compound, depending on its glass transition temperature. The dielectric spectra were collected during heating with a step of $\Delta T = 5$ K below T_g or $\Delta T = 2$ K in the vicinity and above the glass transition.

2.4. X-ray diffraction (XRD)

X-ray diffraction measurements for the studied alcohols were performed at 293 K and then at 143 K, after cooling with a rate of ~2 K/min, on a Rigaku-Denki D/MAX RAPID II-R diffractometer equipped with a rotating Ag anode, an incident beam (002) graphite monochromator, and an image plate in the Debye−Scherrer geometry. The temperature was controlled using an Oxford Cryostream Plus and Compact Cooler. Samples were measured in glass capillaries with a diameter of 1.5 mm. The collected two-dimensional diffraction patterns were converted into one-dimensional intensity data versus the scattering vector, $Q = 4\pi(\sin\theta)/\lambda$, where 2θ is the scattering angle and the wavelength of the incident beam, λ, is equal to 0.56 Å.

2.5. Fourier transform infrared spectroscopy (FTIR)

Fourier transform infrared measurements were carried out using the Thermo Scientific IS50 spectrometer equipped with a standard source and DTGS Peltier-cooled detector. A small amount of alcohol was put between CaF_2 glasses with 1 μm distance to preserve the sample thickness. The spectra were measured in an absorbance mode in the 400–4000 cm^{-1} range. The temperature measurements were performed during cooling using the Linkam heating/cooling stage in the broad temperature range 293–113 K. The spectra were recorded by the accumulation of 32 scans with a spectral resolution of 4 cm^{-1}. The obtained data in post-processing mode were subjected to the baseline, water and carbon dioxide corrections. Finally, in order to separate the α/β and γ/δ bands, the band fitting analysis using Voigt function (convolution of Gaussian-Couchy-Lorentz distributions) was carried out in Grams 9.2. Software Package. During the analysis, the minimum number of components was taken into account to preserve the physical aspect and avoid the problem of random peaks, which might be equated with the unreal situation referred to the studied system. Detailed information on the selection of the minimal number of components was included in Supporting Information. The hydrogen stretching bands were refined with three functions because three separate inputs stemming from α/β OHs, γ OHs and δ OHs were reported on the basis of the difference IR spectra [8]. The applied procedure allowed achieving the correct peak position, intensity, area (integrated intensity), area ratios, and full width at half maximum (*FWHM*). Additionally, the correctness of the fitting procedure was checked by the calculation of the 2-nd derivative.

2.6. Refractometry

The temperature-dependent refractometric measurements of the analyzed set of 1-phenyl alcohols in the liquid phase were carried out with a resolution of 0.0001 by means of the Mettler Toledo refractometer RM40 in the temperature range of 288–353 K. The temperature was controlled by Peltier thermostat with a precision better than 0.1 K.

2.7. Density functional theory (DFT) calculations

The theoretical calculations were performed with the use of the density functional theory in the Gaussian09 program on B3PW91/6-311 g++ level (functional and basis set implemented in the Gaussian09 package) [35,36]. The B3PW91 functional was chosen because it is recommended to describe the electronic properties of organic molecules

[37,38]. The molecular geometry of the singlet ground state of the studied compounds was optimized in the gas phase. Vibrational frequency calculations were performed for each compound to ensure that the optimized geometries represent the local minima of the potential energy surface and that only positive eigenvalues were found.

3. Results and discussion

3.1. Calorimetric studies

All analyzed 1-phenyl alcohols are liquid at room temperature and can be vitrified with ease. No crystallization process was detected for any compound during cooling with a rate of 10 K/min. The subsequent heating scans, also performed with a rate of 10 K/min, revealed the occurrence of the characteristic small thermal effect connected with the glass transition, which takes place in the vicinity of 198 K for 1P1E, 1P1P, 1P1B and 206 K for 2M1P1P (Fig. 2). Noteworthy is that despite differences in molar mass, the linear alcohols are characterized by basically the same glass transition temperature. Change in the molecular shape to a globular one by the branching of the alkyl chain results in an increase in T_g, which is well visible when comparing the isomeric 1P1B and 2M1P1P. Further heating of 1P1E and 1P1B leads to the cold crystallization from the supercooled liquid state, which is evident on the heating thermograms as an exothermic peak with the onset at 234 and 235 K, respectively (Fig. 2). An additional small exothermic peak was detected for 1P1B at ~255 K, suggesting polymorphism of this compound. However, further investigations are required to confirm this assumption. The crystal phases of 1P1E and 1P1B are characterized by the melting points at 255 and 289 K, respectively (Fig. 2). On the other hand, no crystallization process was detected for 1P1P and 2M1P1P on heating. In order to characterize the factors responsible for such calorimetric properties of the 1-phenyl alcohols, the XRD patterns were analyzed.

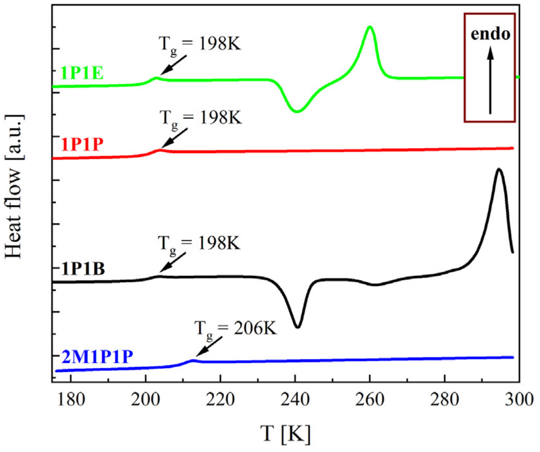

Fig. 2. DSC thermograms of the studied 1-phenyl alcohols collected on heating with a rate of 10 K/min.

3.2. X-ray diffraction studies

The range of diffraction data up to around 2.5 Å^{-1}, presented in Fig. 3, is contributed mainly from the intermolecular correlations in the studied alcohols. Two broad maxima are observed in this region. The main diffraction peak (MP), appearing at $Q_{MP} \approx 1.45$ Å^{-1} at 293 K, is caused by the short-range intermolecular order and corresponds to an average nearest-neighbor intermolecular distance, $d_{MP} = 2\pi/Q_{MP}$, of around 4.3 Å. This length is slightly shifted towards shorter intermolecular distances for 1P1B, and longer distances for 2M1P1P (see Supporting Information for a detailed description of the XRD data analysis and the obtained values of the structural parameters), reflecting the difference in the geometry of these two molecules. At 143 K, that is below the T_g, the maximum of the principal peak shifts towards greater Q for each sample, indicating shortening of the nearest intermolecular distances due to the temperature drop, which is a typical thermal effect. Moreover, the 1P1B crystallizes at 143 K what can be recognized as the appearance of sharp Bragg peaks in the diffraction pattern. In turn, one may observe a transformation of the MP shape for 2M1P1P. Such a change may result from the modification of the mutual arrangement of molecules on the local scale at low temperature, e.g., from the chain-like to ring-like architecture. Besides, the intensity of the MP slightly decreases with temperature for 1P1E, 1P1P and 2M1P1P (for 1P1B crystallization precludes the analysis). This is a non-Debye-Waller behavior, which may support the conception of the temperature-dependent reorganization of the intermolecular structure of these alcohols due to the increase in H bond strength, the ongoing association process and/or formation of a greater number of multimer H-bonded structures. On the other hand, the conformational transformation of molecules, already predicted for 1P1E [34], may also trigger such changes. However, the diffraction data collected for high-Q values up to 20 Å^{-1} and the atomic pair distribution functions calculated based on the data (see Fig. S7 and Fig. S8 in Supporting Information, respectively) do not exhibit any significant temperature-dependent differences in the intramolecular structure of these alcohols. Therefore, this scenario is unlikely in this case.

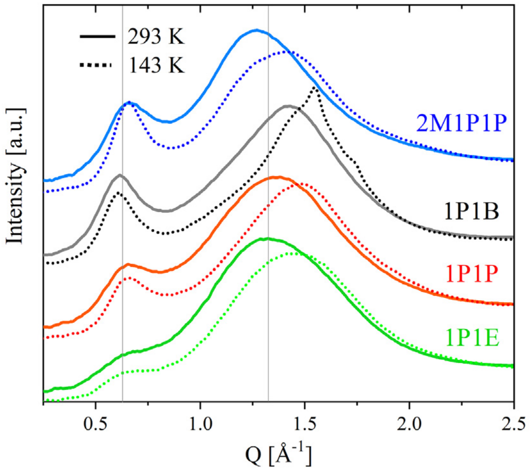

Fig. 3. X-ray diffraction patterns of 1P1E, 1P1P, 1P1B and 1P2M1P in low scattering vector range, at 293 and 143 K.

The diffraction data in the low Q range around 0.6 Å^{-1} exhibits a characteristic pre-peak (PP), differing in the intensity between the studied alcohols (Fig. 3). The appearance of such a characteristic feature is a signature of the spatial organization of molecules on the medium-range length scale that goes beyond the usual short-range liquid order. In various alcohols, the PP is usually assigned to an ordering of the H-bonded supramolecular associates on the length scale of nanometers [8]. The PP integrated intensity is dependent on the degree of the medium-range order (the mean size, homogeneity and number of the organized supramolecular structures). As can be seen, the PP is the lowest for 1P1E and the most intense for 1P1B and 2M1P1P. From the full width at half maximum, *FWHM*, of the MP and PP the average coherence lengths, $L_{mp} = 2\pi/FWHM_{mp}$ and $L_{pp} = 2\pi/FWHM_{pp}$, respectively, may be determined. These parameters are related to the static length scales of the short- and medium-range intermolecular order, respectively. At room temperature, L_{mp} and L_{pp} for 1P1E are around 8 and 16 Å, respectively, (see Table S1 in Supporting Information), suggesting that the supramolecular associates are rather small, mainly dimeric, trimeric, with the intermolecular order limited to around 1–2 nm, as suggested in reference

[34]. L_{mp} of 1P1P and 1P1B is similar to that of 1P1E. However, these three samples have a different ability to organize on the medium-range scale. At 293 K the range of the intermolecular order L_{pp} extends to around 16, 22 and 31 Å, for 1P1E, 1P1P and 1P1B, respectively. Thus, the XRD data confirm the formation of nanosized supramolecular associates in the studied set of phenyl alcohols. For linear alcohols, the longer the alkyl chain, the higher the tendency to intermolecular ordering in the medium-range scale, reflected in the intensities of the pre-peaks and the values of the L_{pp}. The diffraction pre-peaks get sharper for all the studied alcohols at a temperature near T_g, reflecting the formation of greater associates and extension of the medium-range order upon temperature drop. Isomeric 1P1B and 2M1P1P form the biggest supramolecular clusters with the highest degree of the nanoscale order ($L_{pp} \approx 37$ and 31 Å at 293 K, respectively). However, they slightly differ in the average medium-range order distance related to the pre-peak position ($d_{pp} \approx 10.3$ and 9.7 Å at 293 K for 1P1B and 2M1P1P, respectively). To shed more light on this issue, broadband dielectric measurements were performed.

3.3. Dielectric results

Broadband dielectric spectroscopy is a powerful tool that provides information on the molecular dynamics in the supercooled liquid and glassy states and gives an insight into orientational cross-correlations of dipole moments between neighboring molecules in the liquid phase. For this purpose, the analysis of temperature evolution of the Kirkwood-Fröhlich factor, g_k, is used, calculated according to the formula: $g_k = \frac{9k_B\varepsilon_0 MT(\varepsilon_s-\varepsilon_\infty)(2\varepsilon_s+\varepsilon_\infty)}{\rho N_A\mu^2\varepsilon_s(\varepsilon_\infty+2)^2}$, where k_B is the Boltzmann's constant, N_A - Avogadro number, M - molar mass, ε_0 - permittivity of a vacuum, ρ - density, and μ is molecular dipole moment [39]. For the calculations, the values of μ were taken directly from the performed DFT computations (see Table 1).

The temperature evolution of density, $\rho(T)$, was calculated according to the Lorentz-Lorenz equation [40,41], based on the molecular polarizability, α, obtained from DFT computations and a linear extrapolation of temperature measurements of refractive index, $n(T)$ (see Fig. S3 in Supplamentary Information). The $n(T)$ was also used for calculation of the permittivity values at infinite frequencies, ε_∞ ($\varepsilon_\infty \approx n^2$), whereas the temperature evolution of the static values of dielectric permittivity, ε_s, was derived directly from the dielectric spectra of the real part of the complex dielectric permittivity, ε′. Calculations and further analysis of the thermal evolution of g_k were omitted in the case of 1P1B because of its high tendency to undergo crystallization and melting point close to room temperature. The results for the other alcohols are shown in Fig. 4.

The temperature evolution of g_k is fundamentally different when comparing the linear alcohols with the globular one. In the case of the linear 1P1E and 1P1P, the values of g_k are higher than 1 in the whole temperature range and increase when approaching T_g. Taking into account the previously discussed X-ray diffraction studies showing the presence of supramolecular H-bonded clusters in the phenyl alcohols even at room temperature, these findings indicate that the linear 1P1E and 1P1P tend to form chain-like associates and, what is more, the share of cross-correlations of dipole moments involved in the chain-like organization of H bonds increases when lowering the temperature.

Table 1
Glass transition temperature determined from calorimetry ($T_{g\ (DSC)}$), steepness index (m_{100s}), dipole moment (μ) and polarizability (α) of the analyzed 1-phenyl alcohols.

Substance	$T_{g(DSC)}$ [K]	m_{100s}	μ [D]	$\alpha \cdot 10^{-40}$ [C^{2}m^2/J]
1P1E	198(1)	87(2)	1.71	14.43
1P1P	198(1)	73(2)	1.66	16.46
1P1B	198(1)	66(2)	1.65	18.46
2M1P1P	206(1)	67(2)	1.69	18.26

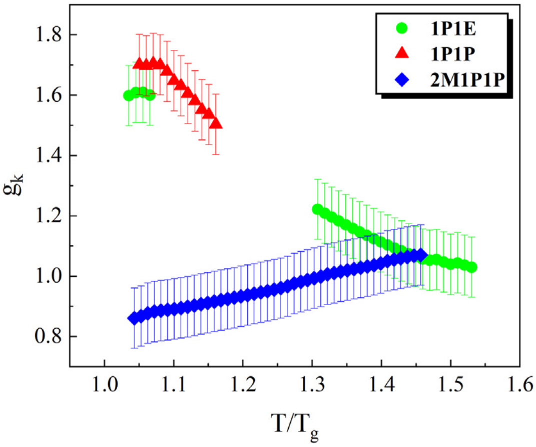

Fig. 4. Temperature dependence of Kirkwood-Fröhlich factor for 1P1E, 1P1P and 2M1P1P.

It should be emphasized that the obtained results for 1P1P are in good agreement with previous studies on this compound [32]. In turn, the Kirkwood-Fröhlich factor of the globular 2M1P1P decreases when approaching the glass transition, taking the values lower than 1. It means that, in contrast to 1P1E and 1P1P, ring-like H-bonded associates are preferable in 2M1P1P when lowering the temperature. This outcome is in good agreement with XRD data, which indicated differences in the morphology of the supramolecular clusters between the linear (1P1E, 1P1P and 1P1B) and globular (2M1P1P) alcohols. Interestingly, for each analyzed alcohol, the values of the Kirkwood-Fröhlich factor tend to ~1 with increase in T. Similar behavior was previously reported for other monohydroxy alcohols [8].

Representative frequency-dependent dielectric loss spectra of the titled phenyl monohydroxy alcohols, ε″(f), registered both above and below the glass transition, are presented in Fig. 5. No relaxation process can be detected at temperatures lower than T_g in the case of 1P1E. On the contrary, one secondary relaxation of a low magnitude is visible for the other 1-phenyl alcohols. The maxima of this process, shifting towards higher frequencies when raising the temperature, are visible much below T_g for 1P1P and 1P1B. In the case of 2M1P1P, the secondary relaxation peaks remain visible also in the vicinity of T_g. However, they become gradually less marked with temperature increase due to overlapping with the main relaxation. Surprisingly, each alcohol is characterized by only a single dominating relaxation peak above T_g (labeled as the main relaxation in Fig. 5), much more pronounced in magnitude and of greater sensitivity to temperature changes than the secondary one. Temperature rise, followed by an acceleration in motions of molecules and the whole H-bonded clusters in the supercooled liquid, may promote the formation of crystallization nuclei leading to the rapid cold crystallization process. Such a phenomenon was observed in the case of 1P1E and 1P1B, what can be seen in the dielectric loss spectra as a significant drop in the amplitude of the main relaxation process (see Fig. 5a and d). The cold crystallization was not observed for 1P1P and 2M1P1P, which is in good agreement with previous works reporting hindrance of crystallization for various phenyl derivatives of propanol [32].

Molecules of all the analyzed 1-phenyl alcohols organize themselves into supramolecular clusters. Therefore, the main relaxation peak should be treated, according to [32], as a combination of the structural α- and Debye processes, connected with the dynamics of single molecules and their aggregates, respectively. Besides, it was previously shown that phenyl alcohols could be characterized by a small separation between the Debye and α-relaxation processes so that they are often merged [32]. To verify if such a scenario happens for the alcohols studied here, the dielectric loss spectra registered above glass transition temperature were refined with the Fourier transform of the

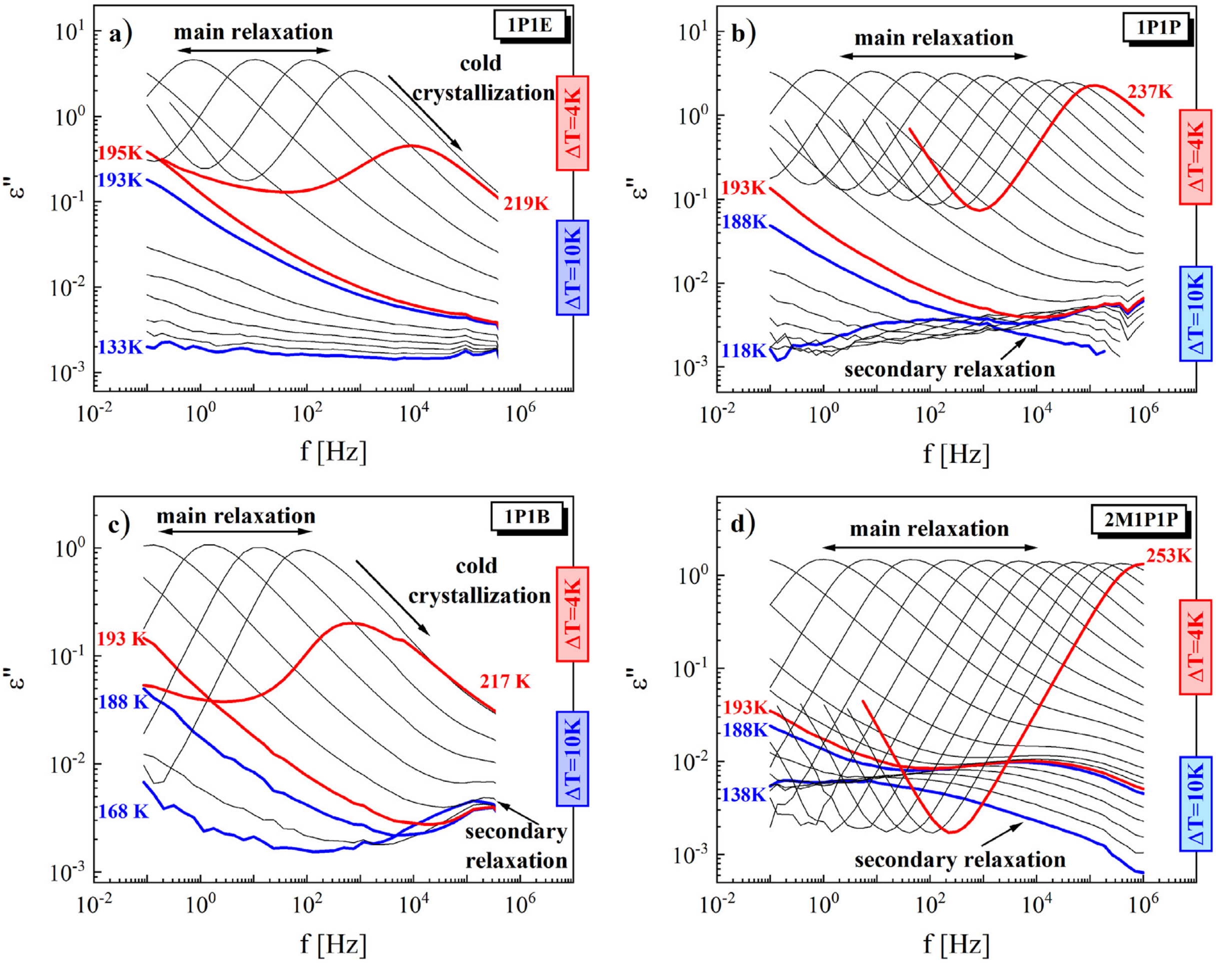

Fig. 5. Selected frequency-dependent dielectric loss spectra of 1P1E (a), 1P1P (b), 1P1B (c) and 2M1P1P (d).

Kohlrausch-Williams-Watts (KWW) function [42]. As shown on the exemplary ε''(*f*) spectrum gathered at 205 K for 1P1E (Fig. 6), the main relaxation peak is described with the KWW function only in the very vicinity of the maximum (Fig. 6). Similar results were also obtained for the other alcohols investigated herein. Based on the temperature dependence of the β_{KWW} factor one should notice that the values of this parameter are smaller than 1 in the whole temperature range for all analyzed monohydroxy 1-phenyl alcohols (see inset in Fig. 6). In the vicinity of T_g, the broadening is considerable for the isomeric 1P1B and 2M1P1P, however, it decreases significantly for the 1P1E and 1P1P. The values of β_{KWW} increase with temperature raise (see inset in Fig. 6), similarly to other previously reported phenyl alcohols, such as 2-phenyl-1-propanol [32]. In the case of 1P1P, the β_{KWW} exceed 0.9 at $T/T_g = 1.14$. On the one hand, the narrowing of the main relaxation peak while temperature raising may indicate that the time-temperature superposition is violated. However, it may also suggest that the peak is a combination of two processes with different temperature dependencies: the low-frequency Debye process and the structural α-relaxation with a maximum located close to the maximum of the Debye mode. It should be stressed that this conception is supported by the previous studies of 1-phenyl-1-propanol by Böhmer et al. [32], as well as our XRD results, thermal evolution of the Kirkwood-Fröhlich coefficient and the fact that the main relaxation peak is poorly described with a single narrow KWW function for each analyzed alcohol.

The significant broadening of the relaxation peak in the case of isomeric 1P1B and 2M1P1P suggests a total disappearance of the Debye process or its much smaller amplitude, leading to a noticeably smaller contribution to the overall relaxation dominated by the structural α-process. Such a scenario is possible when we consider lower concentration, smaller size and/or different architecture of the supramolecular H-bonded associates resulted from the increase in the length of the aliphatic chain and/or its branching. This is highly likely in the case of 2M1P1P which tends to organize itself in ring-like clusters, for

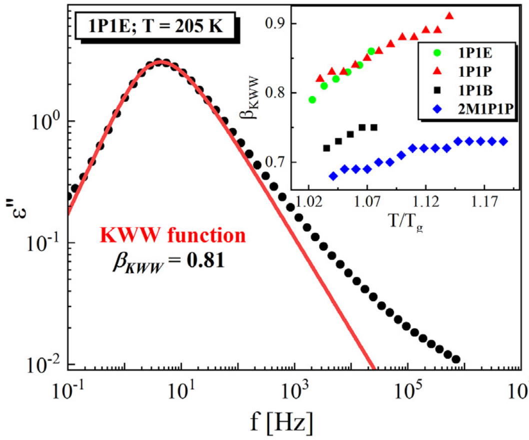

Fig. 6. Dielectric loss spectrum registered for 1P1E at 205 K and refined with KWW function. The inset shows the temperature dependencies of the β_{KWW} parameter for all 1-phenyl alcohols.

which the overall dipole moment is close to 0 D. However, the KWW function does not describe well the high-frequency slope of the relaxation process even for this alcohol (see Fig. S6 in Supplementary Information). Therefore, it cannot be excluded that also chain-like associates are formed by 2M1P1P, being in the thermal equilibrium with the ring-like aggregates. Consequently, the Debye process still may be present in this case, but its amplitude and, consequently, its contribution to the main relaxation peak are much lower in comparison with 1P1E and 1P1P. On the other hand, it can be related only to the contribution of the secondary relaxation process.

To better understand the unobvious dynamic properties of the set of 1-phenyl alcohols and to obtain detailed information on temperature behavior of the relaxation processes, the peaks were described with fitting functions in the frequency domain. Since the relaxation peaks of secondary processes are symmetrical in shape (see Fig. 5), a description with the Cole-Cole fit function (with fixed shape parameter $\beta = 1$ from the Havriliak-Negami equation [43]) was applied. Such a procedure allowed determining the relaxation times, $\tau_{Max,secondary}$. As shown in Fig. 8, the logarithm of $\tau_{Max,secondary}$ increases linearly with temperature inverse for the secondary process of each analyzed alcohol. Therefore, the Arrhenius law was used for parametrization of the temperature dependences, given by the formula: $\tau_{Max,secondary} = \tau_\infty \, exp\left(\frac{E_a}{RT}\right)$, where E_a is the activation energy and R is the gas constant. As shown in Fig. 8, the β-relaxation times of 2M1P1P are much longer (up to 4 decades) in comparison with those of 1P1B and 1P1P. Also the activation energy (33(1) kJ/mol) is much higher for this compound. On the contrary, the temperature dependences of β-relaxation times of 1P1B and 1P1P are similar to each other, being characterized by the same value of activation energy with respect to inaccuracy ~25 kJ/mol. However, the relaxation times are slightly shorter, by about 0.25 decade, for 1P1B. Secondary relaxation processes can be of intra- or intermolecular character. The first ones are connected with rotational motions of molecular fragments. The second ones, associated with limited reorientation of whole molecules, have been named as Johari-Goldstein (JG) type. In order to determine the origin of a secondary relaxation we decided to check the empirical relation proposed by Kudlik et al., which links the activation energy of this process, E_a, with the glass transition temperature: $\frac{E_a}{RT_g} = 24$ [44–46]. Although some deviations were observed, this relation is fulfilled for the vast majority of compounds if the analyzed secondary relaxation process is of JG type [47]. Taking the T_g and E_a determined previously for the analyzed set of 1-phenyl alcohols, the $\frac{E_a}{RT_g}$ ratio takes the value of 15.2(7), 14.6(7) and 19.9(7) for the 1P1P, 1P1B and 2M1P1P, respectively. Although the determined ratio for the latter compound deviates from 24, the value is comparable with those obtained for β-relaxations of JG type for 5-methyl-2-hexanol or 2-ethyl-1-hexanol [47]. Therefore, one can assume that the secondary relaxation process in 2M1P1P belongs to this group. On the other hand, the determined values for 1P1P and 1P1B correspond well to those calculated for γ-relaxations of non-JG type for poly[(phenyl glycidyl ether)-*co*-formaldehyde] (PPGE) or benzoin isobutylether (BIBE) [47], being far lower than 24. The obtained results indicate that the registered secondary relaxations for 1P1P and 1P1B are of intramolecular character, connected with rotational motions of a substituent. Since all analyzed compounds possess a phenyl ring and no γ-relaxation was observed in the case of 1P1E, rotational motions of the aromatic substituent can be excluded from the possible sources of this process. Small amplitude and short relaxation times even at very low temperatures (such as 118 K) indicate that it may originate from reorientational motions of the ends of alkyl chains, that is C_2H_5 and C_3H_7 groups of 1P1P and 1P1B, respectively. Rotation of these moieties, e.g., around the C1-C2 bond, should be fast even at low temperatures and may cause small changes in the value of dipole moment vector, making the rotation possible to be registered via dielectric studies. What is more, rotational motions of a methyl CH_3 group around the C1-C2 bond, leading to changes in conformations between staggered and opposite ones, in the case of 1P1E, are highly unlikely to be observed, what is in good agreement with the obtained results (only α-relaxation process is registered).

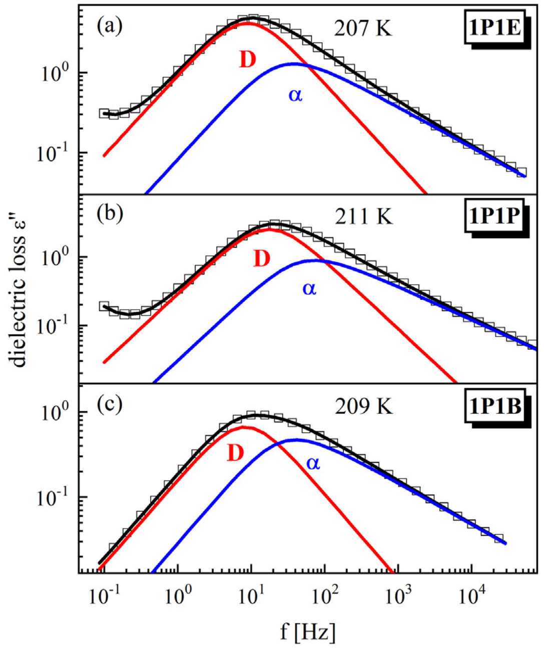

Fig. 7. Selected dielectric loss spectra of 1P1E, 1P1P and 1P1B with added fitting functions of the Debye and α-processes.

In contrast to the secondary relaxation, the main relaxation peaks of 1P1E, 1P1P and 1P1B are asymmetrically broadened and, what is more, contain a considerable kink in the high-frequency slope (Fig. 7). Considering positive cross-corelation between neighboring molecules and values of β_{KWW} parameter close to 1, such a feature suggests that the spectra registered above T_g are a combination of two overlapping processes. Therefore, refinement with a sum of the Cole-Davidson (observed for structural relaxations of numerous mono- and polyhydroxy alcohols such as glycerin, 1-phenyl-2-butanol, 2-phenyl-1-butanol [31,48]) and the Debye functions was applied for the exemplary $\varepsilon''(f)$ spectra of 1P1E, 1P1P and 1P1B. As shown in Fig. 7, the time separation between the maxima of the Debye and structural α-relaxation is less than 1 decade for each alcohol. Such a small value is in good agreement with previous studies on 1P1P based on the combination of PCS and BDS techniques. It should also be emphasized that the time separation between the maxima of the Debye and the main relaxation peaks is basically negligible (is less than 0.1 decade). Therefore, one can suppose that the temperature dependence of the relaxation time determined directly from the main relaxation peak will correspond to the temperature evolution of the Debye process. Such an assumption allow us to avoid possible mistakes, particularly at higher temperatures, connected with a model-dependent fitting procedure due to the too small time-scale separation of the relaxation processes.

Therefore, in order to obtain more precise information on a temperature behavior of the main dielectric process for each compound, the relaxation peaks were described with the Havriliak-Negami (HN) function only in the very vicinity of the maximum: $\varepsilon^*(\omega) = \varepsilon_\infty + \frac{\Delta\varepsilon}{\left[1+(i\omega\tau_{HN})^{1-\alpha}\right]^\beta}$, where ε^* is complex permittivity, $\Delta\varepsilon$ - dielectric strength, ε_∞ - the high-frequency limit of permittivity, ω - angular frequency, τ - the relaxation time, α and β are the shape parameters [43]. For each analyzed compound the α parameter of HN function took the value of 1 in the whole temperature range, transforming the fit function to the Cole-Davidson form. As shown in Fig. 8, the obtained temperature dependence of relaxation times, $\tau_{Max,main}$ in the liquid

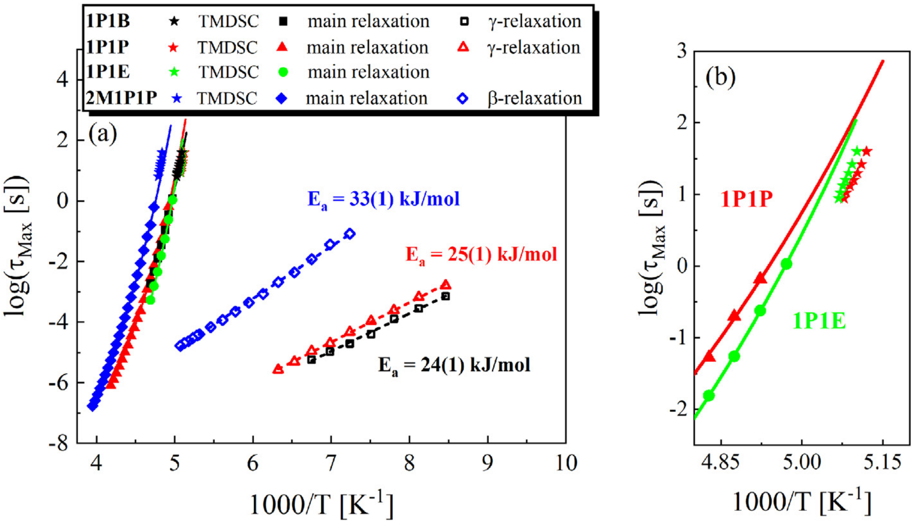

Fig. 8. (a) Relaxation map of the analyzed set of 1-phenyl alcohols. (b) Comparison of the relaxation times obtained from dielectric and calorimetric studies of 1P1E and 1P1P.

phase has a non-linear, super-Arrhenius character for each analyzed alcohol, which can be refined with the Vogel-Fulcher-Tamman-Hesse equation: $\tau_{Max,main} = \tau_\infty \, exp\left(\frac{D_T}{T-T_0}\right)$, where τ_∞ is a relaxation time at an infinitely high temperature, D_T - a material constant, and T_0 denotes to the ideal glass temperature [49–51]. The results from dielectric measurements were also superimposed on the relaxation times obtained from TMDSC. This technique gives a direct insight into the thermal evolution of structural α-process in the vicinity of T_g. As shown in Fig. 8, the TMDSC and dielectric data are in very good agreement (with respect to the inaccuracy stemming from extrapolation) in the case of 2M1P1P. On the other hand, there is a slight discrepancy between the dielectric and calorimetric results for the linear 1P1E, 1P1P and 1P1B (see Fig. 8b). However, the difference is small and does not exceed 0.8 decade for given isothermal conditions. It should be emphasized that a similar finding was obtained previously for 1P1P [32]. These results confirm that the main relaxation peak of 2M1P1P is related to the structural α-process, whereas the Debye mode has a decisive contribution to the main relaxation process in the case of the other studied phenyl alcohols. Its occurrence for the linear alcohols is closely related to their self-organization in chain-like clusters of non-zero dipole moment. The aggregates are small in each case, which leads to a small time-separation and, as a result, difficulty in identification of the Debye peak in the dielectric loss spectra.

Moreover, there is a high degree of similarity between 1P1E, 1P1P and 1P1B in terms of both temperature dependences of α- and Debye relaxation times (Fig. 8). Taking into account basically the same values of T_g, this result may suggest that increase in the number of carbon atoms in the alkyl chain does not significantly affect the molecular dynamics of the substance, at least when the alkyl chain is short. The relaxation times of 2M1P1P (determined form both TMDSC and BDS) differ significantly from the values for the other alcohols, being always slower at each measured temperature. Such an image clearly shows that addition of a side substituent to the alkyl chain (in this case a methyl group), accompanied by a change in the shape of a molecule from linear to more globular, significantly affects the glass transition temperature and the molecular dynamics in the supercooled liquid.

To get a deeper insight into the self-organization phenomenon, the *steepness* index, m, was calculated for the analyzed alcohols. This parameter describes the sensitivity of the relaxation times (and thus the molecular dynamics) to temperature changes when approaching the reference temperature, T_{ref}, and it is defined as a slope of the tangent to the $log_{10}\tau_{Max,\ main} = f(T_{ref}/T)$ curve at the temperature equal to T_{ref} [52]: $m = \left.\frac{d\,log_{10}\tau_{Max,main}}{d\left(T_{ref}/T\right)}\right|_{T=T_{ref}}$. It should be mentioned that although the relaxation times were taken from the thermal evolution of the main relaxation peaks instead of the Debye ones, a negligible time-separation between them allow conducting such an analysis. The reference temperature was defined here as a temperature at which the relaxation time is equal to 100 s. Hence, in order to determine the *steepness* index for each alcohol, the main relaxation times were extrapolated by about two decades. As presented in Table 1, the estimated values of the *steepness* index decrease with an increase in the number of carbon atoms in the alkyl chain of the monohydroxy alcohol from 87(2) for 1P1E, through 73(2) for 1P1P, to 66(2) for 1P1B and 67(2) for the isomeric 2M1P1P. This tendency seems to reflect the behavior of the diffraction pre-peak feature: the higher the values of the pre-peak intensity and width, the lower the *steepness* index. Taking into account that the *steepness* index can also be treated as an indicator of H-bonded supramolecular clusters [31], two scenarios must be taken into account: the size of the suprastructures becomes larger, or their concentration rises as the number of carbon atoms in the alkyl chain of the phenyl alcohol increases. In order to explain the self-assembly phenomenon thoroughly and to characterize the related structural features of the set of 1-phenyl alcohols, particularly the hydrogen-bonding pattern, further studies by means of infrared spectroscopy were performed.

3.4. Infrared spectroscopy studies

In the case of IR measurements the main emphasis was put on the analysis of the high wavenumber 3700–2600 cm^{-1} spectral region because of the origin of bands in this range linked to the stretching ν(OH) modes, as well as the characteristic asymmetric and symmetric stretching vibrations of the CH_x groups ($x = 1,2,3$). A very similar band arrangement with small differences appearing in the 3800-2800 cm^{-1} range results from the variation in the alkyl chain length and branching. As shown in Fig. 9, the IR spectra of each phenyl alcohol measured at 298 K in the liquid phase are characterized by two OH bands centered at 3553 and 3347 cm^{-1} for 1P1E (Fig. 9a), 3547 and 3334 cm^{-1} for 1P1P (Fig. 9b), 3553 and 3353 cm^{-1} for 1P1B (Fig. 9c), 3548 and 3409 cm^{-1} for 2M1P1P (Fig. 9d). According to previous reports, the band with lower intensity located at higher wavenumber stems from stretching vibrations of non-bonded or weakly bonded α OH groups of monomeric molecules in the liquids or β OH groups of terminal molecules of supramolecular structures, in which they play a

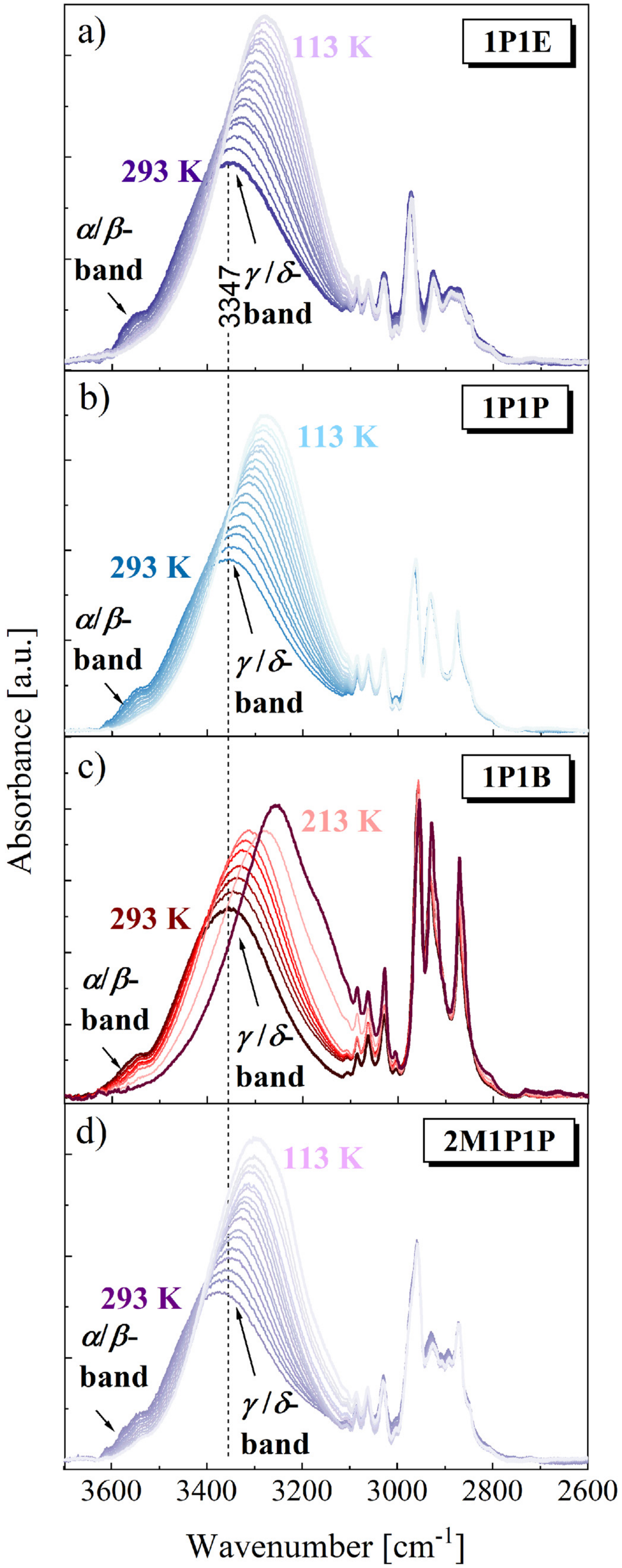

Fig. 9. Infrared spectra of 1P1E (a), 1P1P (b), 1P1B (c) and 2M1P1P (d) in the 3650–2600 cm^{-1} range, measured on cooling with 20 K/min from 293 K down to 113 K.

role of only proton acceptors [8]. Hence, the term of α/β OH groups is connected with hydroxyl units, which do not play the role of proton donors for the interactions via O-H···O scheme. However, one should keep in mind that such hydroxyl groups can still interact with other molecules in the liquid phase. Since these intermolecular contacts are weak, the α/β-band was reported for numerous compounds to appear at similar wavenumbers (that is above 3600 cm^{-1}) compared to the stretching modes of non-bonded OH groups of isolated alcohol molecules in the gas phase or CCl_4 solutions [8,53,54]. For example, the α/β-band of liquid *tert*-butanol and its CCl_4 solution is centered at similar wavenumber (~ 3625 cm^{-1}) [53,54]. In the case of phenyl alcohols, the OH stretching band originating from isolated molecules in dilution or gas phase is also located above 3600 cm^{-1}, e.g., 3647, 3631 and 3616 cm^{-1} for the supersonic jet, Ar matrix and CCl_4 solutions of 1-phenylethanol, respectively [34,55]. However, contrary to *tert*-butanol or other aliphatic alcohols, the less-intense blue-shifted OH band is located much below 3600 cm^{-1} (~ 3550 cm^{-1}) for the non-diluted phenyl alcohols in liquid phase [34,55]. Therefore, it was assigned to the stretching modes of the hydroxyl groups involved into intermolecular OH···π interactions [34]. Nevertheless, it is still not clear whether this band is an image of an additional molecular ordering or is it a result of random interactions of the phenyl ring with α or β hydroxyl units of the monomers or terminal molecules of H-bonded oligomers, respectively. Therefore, in the case of the studied phenyl alcohols we will label this blue-shifted band of lower intensity as α/β-band connected with OH···π interactions.

The second red-shifted band, much stronger in intensity, results from the occurrence of the H-bonded dimers or multimer structures and is associated with stretching modes of OH groups that are simultaneously acceptors and donors of the proton in hydrogen bonds (δ OHs) or play a role of only proton donor in the H-bonded clusters (γ OHs) [8]. The α/β-band is located at similar wavenumber (~3550 cm^{-1}) at room temperature for all analyzed phenyl alcohols, what suggests a similar strength of intermolecular OH···π interactions, independently from the molecular architecture. This statement seems to be reinforced by previous studies on phenyl-substituted butanols, according to which the α/β-band is centered at 3559 cm^{-1} for 1-phenyl-2-butanol and 4-phenyl-1-butanol, and 3560 cm^{-1} for 4-phenyl-2-butanol [55]. Moreover, the occurrence of this band, resulting from weakly or non-H-bonded OH groups, points that the association degree of the analyzed 1-phenyl alcohols is less than 100% at room temperature. The other bands visible in the range of 3200–2800 cm^{-1} are connected with stretching vibrations of aromatic CH and aliphatic CH_3, CH_2 and CH moieties (Fig. 9).

Lowering the temperature from 278 K down to 113 K with a cooling rate of 20 K/min leads to a gradual change in the position and intensity of the bands connected with the stretching ν(OH) modes. For each alcohol, the intensity of the high-wavenumber α/β-band connected with the occurrence of α/β hydroxyl groups was found decreasing with temperature decline (Fig. 9). This band still occurs and is visible in the IR spectra as a shoulder even at temperatures below T_g (Fig. 9). On the other hand, the amplitude of the second ν(OH) stretching band centered at lower wavenumber and resulting mainly from H-bonded multimer structures is gradually increasing with temperature decrease for all 1-phenyl alcohols (Fig. 9). The obtained results clearly suggest rearrangement of molecules within the H-bonded network when approaching T_g, a decrease in the population of the weak intermolecular OH···π and OH···CH interactions, a reduction of the concentration of monomers and, as a consequence, the formation of a greater number of multimer H-bonded structures. This conclusion is supported by the temperature evolution of the Kirkwood-Fröhlich coefficient calculated from dielectric studies, which also suggested the gradual ordering of the molecules through H-bonds with temperature decrease. The temperature-dependent behavior of 1P1B is a little bit different from

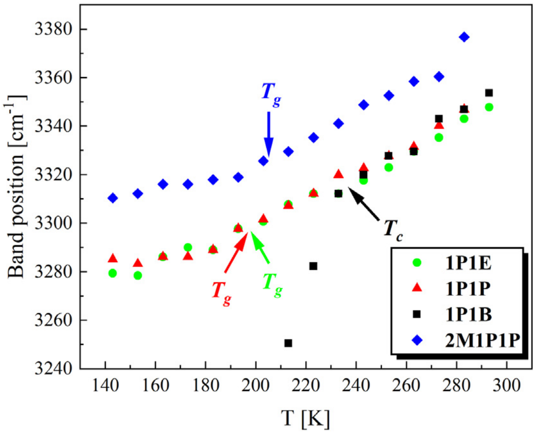

Fig. 10. Temperature dependence of the ν(OH) stretching band position. The glass transition temperatures (T_g) of 1P1E, 1P1P and 2M1P1P and onset of crystallization process (T_c) of 1P1B are marked with arrows.

the other 1-phenyl alcohols. For this compound, the gradual ordering of molecules in liquid with lowering the temperature results in a rapid crystallization process taking place in the vicinity of 223 K even when cooling with a rate of 20 K/min. This phenomenon is visible in the IR spectra as a substantial red-shift of the γ/δ-band (Fig. 9c). The less intense α/β-band, connected with the occurrence of weakly bonded OH groups, vanishes after the crystallization process is completed what suggests that all hydrogen groups are involved in the formation of the 3D network of hydrogen bonding in the crystal lattice.

To provide a more detailed description of the supramolecular association at different thermal conditions, the position of the most intense γ/δ-band was plotted versus temperature (Fig. 10). As a result, a linear shift of the OH band position towards lower wavenumbers is observed when approaching the glass transition: 3347 → 3289 cm^{-1} (1P1E), 3334 → 3289 cm^{-1} (1P1P) and 3409 → 3320 cm^{-1} (2M1P1P). The change in the OH band position is similar for all alcohols and ranges from 0.55 to 0.59 cm^{-1}/K. The red-shift of the γ/δ-band indicates the formation of stronger H bonds due to the shortening of the distance between acceptor and donor atoms while cooling. The formation of H bonds is usually correlated with the transfer of the proton acceptor from the lone pair orbital or π electron system to $\sigma*$(X–H) of the donor (hyperconjugation concept). As a result, the appearance of the H bonding scheme in the molecular system leads to a weakening and slight elongating of the H–X bond. At the same time, the hydrogen bonding Y···H–X (e.g. O···H—O) distance becomes shorter due to stronger molecular interaction [56]. The decrease in the length of the whole O···H—O moieties and thus increase in the strength of hydrogen bonds also takes place during cooling when less thermal energy is delivered to the system in the wake of a reduction in molecular mobility. As a consequence, the main γ/δ OH stretching band observed on the infrared spectrum shifts towards lower wavenumbers. In the vicinity of T_g a kink is observed (Fig. 10), after which the $\nu(\gamma/\delta)$ position red-shifts significantly slower (about 0.2 cm^{-1}/K) towards 3279 cm^{-1} for 1P1E, 3286 cm^{-1} for 1P1P and 3312 cm^{-1} for 2M1P1P at 113 K.

Furthermore, the intensity of the γ/δ band does not undergo significant changes below T_g. This behavior may be justified by freezing of the molecular mobility in glass or occurrence of an equilibrium state in the systems. Fig. 10. also shows that hydrogen bonds are of similar strength for the linear alcohols (1P1E, 1P1P and 1P1B), whereas the more globular 2M1P1P is characterized by weaker H bonds in the whole temperature range. On the other hand, the position of the α/β band, similar for all alcohols at room temperature, does not change significantly while cooling (Fig. 9). It means that the strength of the intermolecular OH···π and OH···CH interactions is almost temperature-independent and similar for the studied compounds at each temperature. Taking into account the previously discussed calorimetric and dielectric results, showing that the linear alcohols are characterized by almost the same value of T_g whereas it is about 8 K higher for the globular 2M1P1P, it demonstrates that the strength of hydrogen bonds have a decisive impact on the value of the glass transition temperature. Apart from gradually decreasing thermal energy, the appearance of stronger H bonds when approaching T_g contributes to the slowdown of the molecular dynamics of the systems. However, considering the similar temperature red-shift of the ν(OH) stretching band for all 1-phenyl alcohols (0.55–0.59 cm^{-1}/K) and different temperature dependences of the relaxation times (see Fig. 8a) one should conclude that there must also be another factor affecting the molecular dynamics of the studied phenyl alcohols in the supercooled liquid state.

As pointed before, the degree of association of molecules via H bonds is less than 100% for each alcohol at both room and low temperatures. Nevertheless, distinct changes are observed while cooling. Moreover, some differences are observed when comparing the IR spectra for these compounds with each other. To enable such a comparison, the IR spectra were normalized so that the intensity of the γ/δ-band is equal to 1. As shown, the α/β-band has the highest intensity for the globular 2M1P1P at room temperature whereas the linear 1P1E and 1P1B are characterized by the lowest one (Fig. 11a). It indicates that the structure of the phenyl alcohol molecule affects not only the type of the formed supramolecular associates (ring- or chain-like) but also the degree of association, which is the lowest in the case of 2M1P1P. It seems that branching of the alkyl chain in the very vicinity of the hydroxyl group plays the role of a steric hindrance for the organization of molecules in supramolecular H-bonded clusters. Cooling of the alcohols down to the temperature close to the glass transition (e.g., 203 K) leads to a considerable increase in the degree of association, which is visible as a decrease in the intensity of the α/β-band (Fig. 11b). At this temperature region, the differences between the alcohols become less pronounced, but 2M1P1P is still the least associated. Further cooling down to 113 K leads to an only slight increase in the ordering of molecules (compare Fig. 11b and c), which is due to freezing of molecular motions in the glassy state.

The temperature-induced changes in the degree of association can be analyzed more precisely in terms of the thermal evolution of the area under the α/β-band, $I_I(\alpha/\beta)$, with respect to the area under the γ/δ band, $I_I(\gamma/\delta)$. As shown in Fig. 12 the $I_I(\alpha/\beta)/I_I(\gamma/\delta)$ ratio decreases with temperature for all alcohols. Nevertheless, the temperature dependences are different for each compound. Due to the crystallization process, 1P1B was excluded from this analysis. The greatest changes while cooling are observed for liquid 2M1P1P, and the kink visible at ~200 K is related to the glass transition. Similar behavior is observed for 1P1P. However, in this case the changes in the liquid phase are smaller. In the case of 1P1E the values of the $I_I(\alpha/\beta)/I_I(\gamma/\delta)$ ratio change in a linear manner with temperature. Taking into account the small variation of $I_I(\alpha/\beta)/I_I(\gamma/\delta)$ for 1P1E (and thus of the degree of association) between 298 K and the temperature close to T_g, accompanied by significant changes in the Kirkwood-Fröhlich factor, one should conclude that the systems become more ordered and hydrogen bonds become more homogenous in terms of strength at low temperatures. This statement is reinforced by the decrease of the band full width at half of the maximum (*FWHM*) of the γ/δ-band when approaching glass transition (Table 2).

A similar effect is observed for the other alcohols. 1P1B is characterized by smaller *FWHM* at room temperature (the most homogenous strength of H bonds) and also by the lowest intensity of the α/β-band among all studied alcohols, which means that this compound is ordered the most in terms of H bonding pattern at 293 K. This results in its particularly high tendency to crystallize while cooling. The similar low intensity of α/β-band (high degree of association) at room temperature was recognized for 1P1E, which also crystallizes. However, its tendency to undergo this process is far much lower compared to 1P1B. Based on

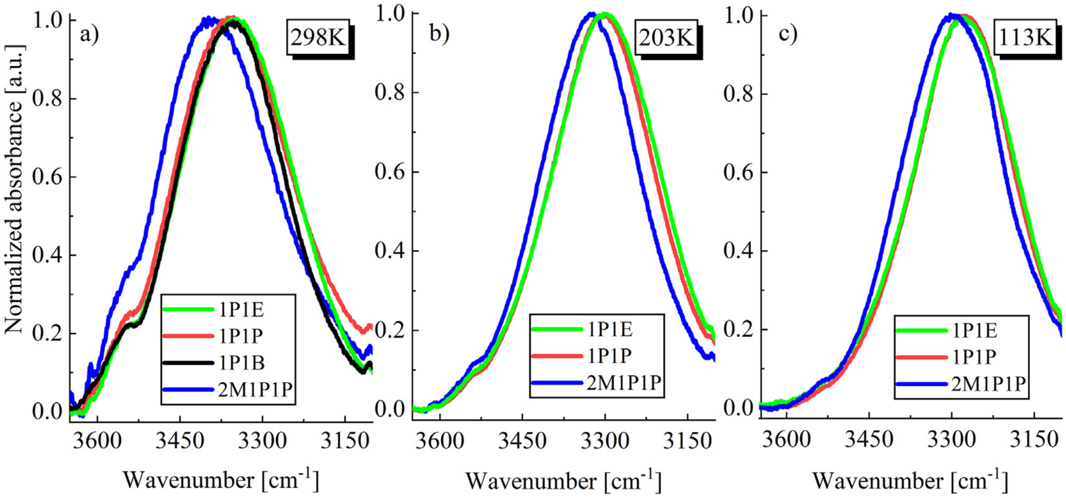

Fig. 11. FTIR spectra of the analyzed 1-phenyl alcohols in the non-crystalline state, in the 3100–3650 cm^{-1} frequency range at 298 K (a), 203 K (b) and 113 K (c). The spectra were normalized to the intensity of γ/δ-band.

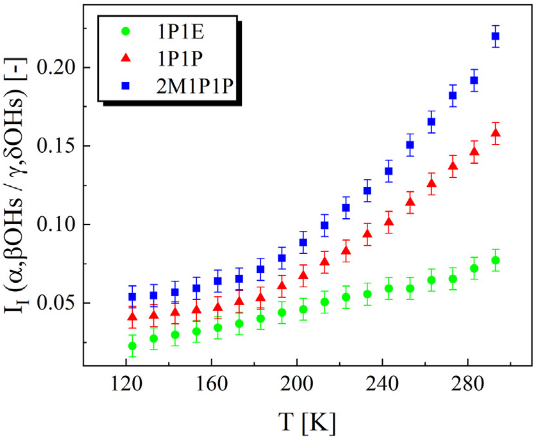

Fig. 12. Thermal evolution of the $I_I(\alpha/\beta)/I_I(\gamma/\delta)$ ratio for 1P1E, 1P1P and 2M1P1P.

this observation, one can conclude that the length of the alkyl chain plays a crucial role in crystallization process and the 1-phenyl alcohols with an even number of carbon atoms (1P1B and 1P1E) are more prone to undergo this phase transition.

The performed IR measurements show that the architecture of molecule plays a crucial role not only in the molecular architecture of the clusters (ring- or chain-like) but also affects the degree of association, strength of intermolecular H bonds and crystallization tendency. Additional branching of the alkyl chain in the vicinity of OH group contributes to a significant reduction of the degree of association and hydrogen bond weakening, while the length of the alkyl chain has a decisive impact on the crystallization tendency. Moreover, IR measurements revealed that the glass transition temperature is controlled mainly by the strength of H bonds, whereas the molecular dynamics in the liquid phase depends on the thermal evolution of H bond strength, degree of association as well as the morphology of supramolecular structures.

Table 2
Comparison of *FWHM* of the γ/δ-band of the studied 1-phenyl alcohols for 298 and 203 K.

Compound	*FWHM* at 298 K [cm^{-1}]	*FWHM* at 203 K [cm^{-1}]
1P1E	243(4)	230(4)
1P1P	254(4)	223(4)
1P1B	232(4)	–
2M1P1P	250(4)	218(4)

4. Conclusions

The influence of the molecular architecture of a set of four 1-phenyl alcohols (1-phenylethanol, 1-phenyl-1-propanol, 1-phenyl-1-butanol and 2-methyl-1-phenyl-1-propanol) on hydrogen-bonding pattern, molecular dynamics, glass transition temperature and relaxation processes was analyzed. It was found that all studied alcohols form H-bonded supramolecular clusters, despite containing a phenyl ring in the most disfavored position. Moreover, the conjunction of calorimetric and IR studies allowed us to determine that the molecular architecture and the strength of intermolecular hydrogen bonds have a decisive impact on the glass transition temperature. 1P1E, 1P1P and 1P1B, characterized by a more linear shape of molecules, have a similar strength of hydrogen bonds at each temperature and comparable glass transition temperature. The T_g was determined to be 198 K for these three alcohols. The change in the shape of the alcohol molecules from linear to globular (by the introduction of an additional methyl side group to the alkyl chain), as it is in the case of 2M1P1P, leads to a significant weakening of HBs and an increase in T_g to 206 K. Molecular architecture also affects the vitrification abilities of the 1-phenyl alcohols. However, the length of the alkyl chain plays a crucial role in this case. Similarly to other phenyl derivatives of propanol studied in literature before, two propanol derivatives, 1P1P and 2M1P1P, were found to be good glass-formers, whereas 1P1E and 1P1B showed a tendency to undergo crystallization.

Temperature-dependent dielectric studies of the 1-phenyl alcohols enabled us to observe relaxation processes both above and below the glass transition temperature. Only single secondary relaxation was detected in the glass phase of 1P1P, 1P1B and 2M1P1P. This process was found to be of intramolecular origin for the first two compounds, connected most probably with rotational motions of C_2H_5 and C_3H_7 moieties, respectively. The activation energies of this relaxation are similar for both alcohols, taking the value close to 25 kJ/mol. However, the relaxation times are slightly shorter by about 0.25 decade in the case of 1P1B. Although a single relaxation process seems to occur in the supercooled liquid phase, further refinement with the KWW function brought us to the conclusion that the relaxation peaks are a combination of the Debye and structural α-processes. This statement was reinforced by X-ray diffraction studies, which showed for each 1-phenyl alcohol the occurrence of a pre-peak characteristic for the presence of supramolecular structures where molecules order on the nanoscale. Further studies by means of broadband dielectric spectroscopy allowed us to conclude that the molecular dynamics of the alcohols in the liquid state is not only affected by the intramolecular architecture and hydrogen bond strength but also depends on the morphology (concentration, size and architecture) of the H-bonded associates. Here, a decrease in the *steepness* index with an increase in the number of carbon atoms in the alkyl chain of the linear monohydroxy alcohol was observed. This tendency is in good agreement with the changes in the diffraction pre-peak intensity and *FWHM*. The pre-peak is the least intense and the widest for 1P1E, while for 1P1B it is sharper and has higher intensity, indicating that the isomeric compounds organize into greater supramolecular clusters with a higher degree of the nanoscale order. However, the architecture of the molecules, particularly the location of the steric hindrance, affects the mutual arrangement of molecules in the clusters and the structure of H bond network significantly. The linear 1-phenyl alcohols (1P1E, 1P1P, 1P1B) form preferably chain-like H bond connections, whereas globular-shaped 2M1P1P – ring-like structures. Temperature analysis of the Kirkwood-Fröhlich factor points out that both types of supramolecular structures are in equilibrium at higher temperatures. However, at lower temperatures, linear molecules tend to form bigger and more ordered chain-like structures while globular molecules prefer to arrange into ring-like associates.

Declaration of Competing Interest

There are no conflicts to declare.

Acknowledgments

K.J. is grateful for the financial support from the Foundation for Polish Science within the START program. K.G. is deeply grateful for the financial support from the National Science Centre (Poland) within the framework of the MAESTRO 10 project (Grant No. 2018/30/A/ST3/00323). M. D. is thankful for the financial support from the National Science Center based on decision 2017/26/D/ST8/01117. The research was supported in part by PL-Grid Infrastructure.

Appendix A. Supplementary data

Supplementary data to this article can be found online at https://doi.org/10.1016/j.molliq.2021.115349.

References

[1] G.R. Desiraju, T. Steiner, The Weak Hydrogen Bond in Structural Chemistry and Biology, Oxford University Press Inc., New York, 1999.

[2] S.J. Grabowski, Hydrogen Bonding – New Insights, Springer, Dordrecht, 2006.

[3] T. Steiner, The hydrogen bond in the solid state, Angew. Chem. Int. Ed. 41 (2002) 48–76, https://doi.org/10.1002/1521-3773(20020104)41:1<48::AID-ANIE48>3.0.CO;2-U.

[4] K. Dong, S. Zhang, J. Wang, Understanding the hydrogen bonds in ionic liquids and their roles in properties and reactions, Chem. Commun. 52 (2016) 6744–6764, https://doi.org/10.1039/C5CC10120D.

[5] E.D. Głowacki, M. Irimia-Vladu, S. Bauer, N.S. Sariciftci, Hydrogen-bonds in molecular solids – from biological systems to organic electronics, J. Mater. Chem. B 1 (2013) 3742–3753, https://doi.org/10.1039/C3TB20193G.

[6] A. Guerrero-Corella, F. Esteban, M. Iniesta, A. Martín-Somer, M. Parra, S. Díaz-Tendero, A. Fraile, J. Alemán, 2-Hydroxybenzophenone as a chemical auxiliary for the activation of ketiminoesters for highly enantioselective addition to nitroalkenes under bifunctional catalysis, Angew. Chem. 130 (2018) 5448–5452, https://doi.org/10.1002/ange.201800435.

[7] V. Crupi, S. Magazu, G. Maisano, D. Majolino, P. Migliardo, S. Venuto, Dynamical evidence of aggregates in isomeric alcohols mixtures by O-H stretching band analysis, Phys. Chem. Liq. 26 (1994) 263–272, https://doi.org/10.1080/00319109408029499.

[8] R. Böhmer, C. Gainaru, R. Richert, Structure and dynamics of monohydroxy alcohols-milestones towards their microscopic understanding, 100 years after Debye, Phys. Rep. 545 (2014) 125–195, https://doi.org/10.1016/j.physrep.2014.07.005.

[9] K. Jurkiewicz, B. Hachuła, E. Kamińska, K. Grzybowska, S. Pawlus, R. Wrzalik, K. Kamiński, M. Paluch, Relationship between nanoscale supramolecular structure, effectiveness of hydrogen bonds, and appearance of debye process, J. Phys. Chem. C 124 (2020) 2672–2679, https://doi.org/10.1021/acs.jpcc.9b09803.

[10] A. Jędrzejowska, S. Hensel-Bielówka, K. Koperwas, K. Jurkiewicz, K. Chmiel, J. Jacquemin, D. Kruk, M. Paluch, Peculiar relaxation dynamics of propylene carbonate derivatives, J. Chem. Phys. 150 (2019), 044504, https://doi.org/10.1063/1.5055204.

[11] J.N.A. Canongia Lopes, A.A.H. Pádua, Nanostructural organization in ionic liquids, J. Phys. Chem. B 110 (2006) 3330–3335, https://doi.org/10.1021/jp056006y.

[12] M. Tarnacka, A. Chrobok, K. Matuszek, D. Neugebauer, R. Bielas, S. Golba, K. Wolnica, M. Dulski, K. Kaminski, M. Paluch, Studies on the radical polymerization of monomeric ionic liquids: nanostructure ordering as a key factor controlling the reaction and properties of nascent polymers, Polym. Chem. 7 (2016) 6363–6374, https://doi.org/10.1039/C6PY01274D.

[13] C. Gainaru, R. Figuli, T. Hecksher, B. Jakobsen, J.C. Dyre, M. Wilhelm, R. Böhmer, Shear-modulus investigations of monohydroxy alcohols: evidence for a short-chain-polymer rheological response, Phys. Rev. Lett. 112 (2014), 098301, https://doi.org/10.1103/PhysRevLett.112.098301.

[14] J. Gabriel, F. Pabst, A. Helbling, T. Böhmer, T. Blochowicz, Nature of the Debye-process in monohydroxy alcohols: 5-methyl-2-hexanol investigated by depolarized light scattering and dielectric spectroscopy, Phys. Rev. Lett. 121 (2018), 035501, https://doi.org/10.1103/PhysRevLett.121.035501.

[15] Y. Wang, P.J. Griffin, A. Holt, F. Fan, A.P. Sokolov, Observation of the slow, Debye-like relaxation in hydrogen-bonded liquids by dynamic light scattering, J. Chem. Phys. 140 (2014) 104510, https://doi.org/10.1063/1.4867913.

[16] C. Gainaru, R. Meier, S. Schildmann, C. Lederle, W. Hiller, E.A. Rössler, R. Böhmer, Nuclear-magnetic-resonance measurements reveal the origin of the debye process in monohydroxy alcohols, Phys. Rev. Lett. 105 (2010) 258303, https://doi.org/10.1103/PhysRevLett.105.258303.

[17] S. Pawlus, M. Paluch, M. Dzida, Molecular dynamics changes induced by solvent in 2-ethyl-1-hexanol, Phys. Rev. E 84 (2011), 031503, https://doi.org/10.1103/PhysRevE.84.031503.

[18] L.P. Singh, R. Richert, Watching hydrogen-bonded structures in an alcohol convert from rings to chains, Phys. Rev. Lett. 109 (2012) 167802, https://doi.org/10.1103/PhysRevLett.109.167802.

[19] A.R. Young-Gonzales, R. Richert, Field induced changes in the ring/chain equilibrium of hydrogen bonded structures: 5-methyl-3-heptanol, J. Chem. Phys. 145 (2016), 074503, https://doi.org/10.1063/1.4961022.

[20] S. Pawlus, M. Wikarek, C. Gainaru, M. Paluch, R. Böhmer, How do high pressures change the debye process of 4-methyl-3-heptanol? J. Chem. Phys. 139 (2013), 064501, https://doi.org/10.1063/1.4816364.

[21] M. Wikarek, S. Pawlus, S.N. Tripathy, A. Szulc, M. Paluch, How different molecular architectures influence the dynamics of H-bonded structures in glass-forming monohydroxy alcohols, J. Phys. Chem. B 120 (2016) 5744–5752, https://doi.org/10.1021/acs.jpcb.6b01458.

[22] G.P. Johari, W. Dannhauser, Dielectric study of intermolecular association in sterically hindered octanol isomers, J. Phys. Chem. A 72 (1968) 3273–3276, https://doi.org/10.1021/j100855a030.

[23] T. Hecksher, B. Jakobsen, Communication: supramolecular structures in monohydroxy alcohols: insights from shear-mechanical studies of a systematic series of octanol structural isomers, J. Chem. Phys. 141 (2014) 101104, https://doi.org/10.1063/1.4895095.

[24] W. Dannhauser, Dielectric study of intermolecular association in isomeric octyl alcohols, J. Chem. Phys. 48 (1968) 1911–1917, https://doi.org/10.1063/1.1668989.

[25] J. Lehtola, M. Hakala, K. Hämäläinen, Structure of liquid linear alcohols, J. Phys. Chem. B 114 (2010) 6426–6436, https://doi.org/10.1021/jp909894y.

[26] K.S. Vahvaselkä, R. Serimaa, M. Torkkeli, Determination of liquid structures of the primary alcohols methanol, ethanol, 1-propanol, 1-butanol and 1-octanol by x-ray scattering, J. Appl. Crystallogr. 28 (1995) 189–195, https://doi.org/10.1107/S0021889894010149.

[27] P.P. Nath, S. Sarkar, P.S.R. Krishna, R.N. Joarder, Molecular conformation and structural correlations of liquid D-*tert*-butanol at room temperature by neutron diffraction, Z. Naturforsch. 56 (a) (2001) 825–831.

[28] P.P. Nath, S. Sarkar, P.S.R. Krishna, R.N. Joarder, Intermolecular structure of liquid D-*tert*-butanol by neutron-diffraction data, Appl. Phys. A Mater. Sci. Process. 74 (2002) S348–S351, https://doi.org/10.1007/s003390201546.

[29] G.P. Johari, W. Dannhauser, Dielectric properties of isomeric phenyl propanols, Phys. Chem. Liq. 3 (1972) 1–11, https://doi.org/10.1080/00319107208084084.

[30] G.P. Johari, O.E. Kalinovskaya, J.K. Vij, Effects of induced steric hindrance on the dielectric behavior and H bonding in the supercooled liquid and vitreous alcohol, J. Chem. Phys. 114 (2001) 4634–4642, https://doi.org/10.1063/1.1346635.

[31] S. Kołodziej, J. Knapik-Kowalczuk, K. Grzybowska, A. Nowok, S. Pawlus, Essential meaning of high pressure measurements in discerning the properties of monohydroxy alcohols with a single phenyl group, J. Mol. Liq. 305 (2020) 112863, https://doi.org/10.1016/j.molliq.2020.112863.

[32] T. Böhmer, J.P. Gabriel, T. Richter, F. Pabst, T. Blochowicz, Influence of molecular architecture on the dynamics of H-bonded supramolecular structures in phenyl-propanols, J. Phys. Chem. B 123 (2019) 10959–10966, https://doi.org/10.1021/acs.jpcb.9b07768.

[33] G.P. Johari, O.E. Kalinovskaya, J.K. Vij, Effects of induced steric hindrance on the dielectric behavior and H bonding in the supercooled liquid and vitreous alcohol, J. Chem. Phys. 114 (2001) 4634–4642, https://doi.org/10.1063/1.1346635.

[34] K. Shin-ya, H. Sugeta, S. Shin, Y. Hamada, Y. Katsumoto, K. Ohno, Absolute configuration and conformation analysis of 1-phenylethanol by matrix-isolation infrared and vibrational circular dichroism spectroscopy combined with density functional theory calculation, J. Phys. Chem. A 111 (2007) 8598–8605, https://doi.org/10.1021/jp068448v.

[35] A.D. Becke, Density-functional exchange-energy approximation with correct asymptotic behavior, Phys. Rev. A 38 (1988) 3098–3100, https://doi.org/10.1103/PhysRevA.38.3098.

[36] C. Lee, W. Yang, R.G. Parr, Development of the Colle-Salvetti correlation-energy formula into a functional of the electron density, Phys. Rev. B 37 (1988) 785–788, https://doi.org/10.1103/PhysRevB.37.785.

[37] J. Tomasi, B. Mennucci, R. Cammi, Chem. Rev. 105 (2005) 2999–3094, https://doi.org/10.1021/cr9904009.

[38] J.L. Borioni, M. Puiatti, D. Mariano, A. Vera, A.B. Pierini, In search of the best DFT functional for dealing with organic anionic species, Phys. Chem. Chem. Phys. 19 (2017) 9189–9198, https://doi.org/10.1039/C6CP06163J.

[39] P. Bordewijk, On the relationship between the Kirkwood correlation factor and the dielectric permittivity, J. Chem. Phys. 73 (1980) 595–596, https://doi.org/10.1063/1.439841.

[40] H.A. Lorentz, Ueber die Beziehung zwischen der Fortpflanzungsgeschwindigkeit des Lichtes und der Körperdichte, Ann. Phys. 245 (1880) 641–665, https://doi.org/10.1002/andp.18802450406.

[41] L. Lorenz, Ueber die Refractionsconstante, Ann. Phys. 247 (1880) 70–103, https://doi.org/10.1002/andp.18802470905.

[42] G. Williams, D.C. Watts, Non-symmetrical dielectric relaxation behaviour arising from a simple empirical decay function, Trans. Faraday Soc. 66 (1970) 80–85, https://doi.org/10.1039/TF9706600080.

[43] S. Havriliak, S. Negami, A complex plane representation of dielectric and mechanical relaxation processes in some polymers, Polymer 8 (1967) 161–210, https://doi.org/10.1016/0032-3861(67)90021-3.

[44] A. Kudlik, C. Tschirwitz, S. Benkhof, T. Blochowicz, E. Rössler, Slow secondary relaxation process in supercooled liquids, Europhys. Lett. 40 (1997) 649–654, https://doi.org/10.1209/epl/i1997-00518-y.

[45] A. Kudlik, C. Tschirwitz, T. Blochowicz, S. Benkhof, E. Rössler, Slow secondary relaxation in simple glass formers, J. Non-Cryst. Solids 235–237 (1998) 406–411, https://doi.org/10.1016/S0022-3093(98)00510-9.

[46] A. Kudlik, S. Benkhof, T. Blochowicz, C. Tschirwitz, E. Rössler, The dielectric response of simple organic glass formers, J. Mol. Struct. 479 (1999) 201–218, https://doi.org/10.1016/S0022-2860(98)00871-0.

[47] K.L. Ngai, S. Capaccioli, Relation between the activation energy of the Johari-Goldstein β relaxation and T_g of glass formers, Phys. Rev. E 69 (2004), 031501, https://doi.org/10.1103/PhysRevE.69.031501.

[48] D.W. Davidson, R.H. Cole, Dielectric relaxation in glycerol, propylene glycol, and n-propanol, J. Chem. Phys. 19 (1951) 1484, https://doi.org/10.1063/1.1748105.

[49] H. Vogel, The law of the relation between the viscosity of liquids and the temperature, Phys. Z. 22 (1921) 645–646.

[50] G.S. Fulcher, Analysis of recent measurements of the viscosity of glasses, J. Am. Ceram. Soc. 8 (1925) 339–355, https://doi.org/10.1111/j.1151-2916.1992.tb05536.x.

[51] V.G. Tamman, W. Hesse, Die Abhängigkeit der Viscosität von der Temperatur bei unterkühlten Flüssigkeiten, Z. Anorg. Allg. Chem. 156 (1926) 245–257, https://doi.org/10.1002/zaac.19261560121.

[52] C.A. Angell, Formation of glasses from liquids and biopolymers, Science 267 (1995) 1924–1935, https://doi.org/10.1126/science.267.5206.1924.

[53] P. Kalhor, Q.-Z. Li, Y.-Z. Zheng, Z.-W. Yu, Is the Fourier transform infrared free-OH band of *t*-butanol only from free OHs? Case studies on the binary systems of the alcohol with CCl_4 and $CHCl_3$, J. Phys. Chem. A 124 (2020) 6177–6185, https://doi.org/10.1021/acs.jpca.0c03463.

[54] J.-M. Andanson, J.-C. Soetensa, T. Tassaing, M. Besnard, Hydrogen bonding in supercritical *tert*-butanol assessed by vibrational spectroscopies and molecular-dynamics simulations, J. Chem. Phys. 122 (2005) 174512, https://doi.org/10.1063/1.1886730.

[55] K. Jurkiewicz, S. Kołodziej, B. Hachuła, K. Grzybowska, M. Musiał, J. Grelska, R. Bielas, A. Talik, S. Pawlus, K. Kamiński, M. Paluch, Interplay between structural static and dynamical parameters as a key factor to understand peculiar behaviour of associated liquids, J. Mol. Liq. 319 (2020) 114084, https://doi.org/10.1016/j.molliq.2020.114084.

[56] A.Y. Li, Chemical origin of blue- and redshifted hydrogen bonds: Intramolecular hyperconjugation and its coupling with intermolecular hyperconjugation, J. Chem. Phys. 126 (2007) 154102, https://doi.org/10.1063/1.2715561.